

ORIGINAL ARTICLE

Hazard and Beyond: Exploring Five Distributional Representations of Accelerometry Data for Disability Discrimination in Multiple Sclerosis

Pratim Guha Niyogi*¹ | Muraleetharan Sanjayan² | Dmitri Volfson³ | Kathryn C. Fitzgerald^{2,4} | Ellen M. Mowry^{2,4} | Vadim Zipunnikov¹

¹Department of Biostatistics, Johns Hopkins University, Baltimore, MD, USA

²Department of Neurology, Johns Hopkins University, Baltimore, MD, USA

³Statistical and Quantitative Sciences, Takeda Development Center Americas, Inc, Cambridge, MA, USA

⁴Department of Epidemiology, Johns Hopkins University, Baltimore, MD, USA

Correspondence

*Pratim Guha Niyogi,
Email: pnyogi1@jhmi.edu

Present address

615 North Wolfe Street, Baltimore, MD, 21205.

Abstract

Research on modeling the distributional aspects in sensor-based digital health (sDHT) data has grown significantly in recent years. Most existing approaches focus on using individual-specific density or quantile functions. However, there has been limited exploration to assess the practical utility of alternative distributional representations in clinical contexts collecting sDHT data.

This study is motivated by accelerometry data collected on 246 individuals with multiple sclerosis (MS) representing a wide range of disability (Expanded Disability Status Scale, EDSS: 0-7). We consider five different individual-level distributional representations of minute-level activity counts: density, survival, hazard, quantile, and total time on test functions. For each of the five distributional representations, scalar-on-function regression fits linear discriminators for binary and continuously measured MS disability, and cross-validated discriminatory performance of these linear discriminators is compared across.

The results show that individual-level hazard functions provide the highest discriminatory accuracy, more than double the accuracy compared to density functions. Individual-level quantile functions provided the second-highest discriminatory accuracy. These findings highlight the importance of focusing on distributional representations that capture the tail behavior of distributions when analyzing digital health data, especially in clinical contexts.

KEY WORDS

Distributional representation; scalar-on-function regression, total time on test, hazard function, physical activity

1 | INTRODUCTION

Sensor-based digital health technologies (sDHTs) continuously collect vast amounts of rich and complex data on individual behaviors and health. sDHT data including continuously-monitored physical activity, heart rate, glucose levels, is often heterogeneous across individuals. Traditional modeling approaches methods summarize sDHTs data into simple scalar measures such as total activity count, average heart rate, or total daily steps. To better capture the full individual-specific variability provided by digital health technologies, “distributional data analysis” became a popular alternative (Petersen & Müller, 2019; Ghosal et al., 2021).

In distributional data modeling, instead of reducing data to summary statistics, each individual’s data is represented as a distribution, capturing the variability of their epoch-level sDHT data over the assessment period. Thus, individual-level distributions of sDHT data can serve as outcomes, predictors, or both in regression frameworks known as “distribution regression” (Oliva et al., 2013; Petersen & Müller, 2016; Szabó et al., 2016; Fang et al., 2020; Chen et al., 2021).

In many clinical studies of multiple sclerosis (MS)—a chronic neurological disease affecting the central nervous system—scientists often study the association between disability and ambulatory physical activity assessed via wearable accelerometry (Ezeugwu et al., 2015; Abbadessa et al., 2021; Keller et al., 2022). The most commonly used summary measures for physical activity include total log activity counts, minutes of moderate-to-vigorous-intensity physical activity, and active-to-moderate sedentary transition probabilities (Leroux et al., 2019; Smirnova et al., 2020). As discussed above, these scalar measures ignore the distributional aspect of accelerometry data.

The analysis of distributional data typically relies on classical functional analysis tools, with density functions representing distributions. However, densities are rarely fully observed. Almost always there is a random sample of data, and the density must be estimated using common methods such as kernel density estimation (Póczos et al., 2013; Oliva et al., 2013). Some functional compositional methods for analyzing samples of densities were developed by Petersen & Müller (2016) and Hron et al. (2016). It is well known that due to the boundary effect (Petersen & Müller, 2016), kernel density estimation methods often perform inadequately. Later, Augustin et al. (2017) proposed methods that summarized individual-level distributions via histograms. These distributional representations were used as covariates in linear regression models. Intuitively, discretizing histograms and estimating additional tuning parameters may introduce discrepancies in parameter selection steps.

Chen et al. (2021) and Ghodrati & Panaretos (2022) proposed distribution-on-distribution regression models utilizing Wasserstein distances and optimal transport ideas. Talská et al. (2021) developed a compositional scalar-on-function regression approach using a centered log-ratio transformation of subject-specific densities. This involves mapping densities from the Bayes space of density functions to a Hilbert L_2 space and applying traditional functional data modeling. Matabuena et al. (2021) suggested using subject-specific densities of glucose measures, obtained through continuous glucose monitoring, as predictors and responses. They demonstrated the advantages of this approach over the use of summary measures typically employed in continuous glucose monitoring studies by developing a non-parametric kernel functional regression model using a 2-Wasserstein distance to model scalar outcomes and glucose density predictors.

Yang et al. (2020) proposed quantile-function-on-scalar regression approaches for modeling quantile functions as outcomes, though this approach imposes constraints requiring the regression approximant to be a valid quantile function. Recently, Ghosal et al. (2021) proposed a scalar-on-functional regression framework using subject-specific quantile functions as predictors, while also employing a generalized additive model to capture possible non-linear effects of quantile functions. In contrast to nonlinear space analyses of density functions (Talská et al., 2021) and nonparametric methods using distances or kernels (Matabuena & Petersen, 2021), the approach of Ghosal et al. (2021) is semi-parametric, offering direct interpretability based on subject-specific distributions at quantile levels. Recently, Petersen et al. (2022) provided a comprehensive review of the latest developments in this area in a tutorial-style format.

In reliability and survival analysis, non-negative random variables arise in a wide variety of applications. Mathematical functions such as the distribution function, survival function, density, hazard rates, and total time on test are useful for characterizing probabilistic properties, each with different interpretations (see Marshall & Olkin (2007); Nair et al. (2013) for more details). Although there have been isolated instances where the replacement of distribution functions with the other aforementioned functions has been attempted, systematic comparison has not been done. The main contribution of this article is comparing five distributional representations of minute-level activity counts and demonstrating significantly stronger clinical utility of hazard function, the distributional representation that has received relatively little attention in literature.

The article is organized as follows. In Section 2, we discuss the motivation study of multiple sclerosis. In Section 3, we discuss five different distributional representations and illustrate the proposed methodology. Section 4 provides a detailed statistical analysis. Finally, in Section 5, we conclude with a discussion of the findings, limitations, and potential future directions.

2 | HEAL-MS STUDY

In this section, we present a motivating example and discuss a study conducted within the Johns Hopkins MS Precision Medicine Center of Excellence, which aimed to better understand the manifestation of disability in multiple sclerosis (MS) represented in ambulatory physical activity assessed via wearable accelerometers.

The study was conducted at Johns Hopkins University from January 2021 to March 2023 as part of the Home-based Evaluation of Actigraphy to Predict Longitudinal Function in Multiple Sclerosis (HEAL-MS) project (Rjeily et al., 2022; Tian et al., 2020). MS is a complex neurological disorder affecting the brain and spinal cord, with diverse symptoms that can severely impact quality of life. In early MS, the myelin sheath around axons in the central nervous system is attacked, while later in the course, there is degeneration of the axons themselves. It is this latter process that is thought to underlie the slowly worsening disability

that affects many with MS, known as “progressive” MS. The Expanded Disability Status Scale (EDSS) is a standard clinical tool for measuring MS disability, ranging from 0 (normal neurological function) to 10. Scores from 1.0 to 3.5 indicate good mobility (“low EDSS”), while scores of 4 or higher signify loss of mobility (“high EDSS”).

The study’s goal was to explore the relationship between EDSS scores and ambulatory physical activity. Participants wore accelerometers (GT9X Actigraph) on their non-dominant wrist for two weeks. Raw data were collected at a 30Hz sampling rate, processed using ActiLife v6.134 Lite, and summarized via minute-level activity counts. For the purpose of this study, we focused on the 12 hours of typical wake time that was defined as the period between 8am to 8pm. To account for skewness, we compare both the original activity counts and their log-transformed version defined by $x \rightarrow \log(x + 1)$ transformation.

The analysis included 246 participants, all aged at least 40 (mean age 54.8 years, SD 8.6, 70.7% are female), with no known comorbidities affecting physical activity. Of the sample, 158 participants (64%) with an average age of 53.8 (8.3) had low EDSS scores, and 88 (36%) had high EDSS scores with average age of 56.8 (8.7). Moreover, 113 (71.5%) and 61 (69.3%) are female for the groups low and high EDSS respectively.

3 | MODELING FRAMEWORKS

In the following subsections, we discuss five distributional representations, how each of them are estimated from sDHT data and how those distributional representations are used in scalar-on-distribution functional regression.

3.1 | Five distributional representations

Let random density is a measurable map $f : (\Omega, \mathcal{S}, P) \rightarrow (\mathcal{D}, \mathcal{B}_{\mathcal{D}})$ where (Ω, \mathcal{S}, P) is a probability space and $\mathcal{B}_{\mathcal{D}}$ contains the Borel sets on (\mathcal{D}, d) . We assume that a sample of independent and identically distributed random densities f_i is available for regression analysis, but in reality, we observe them rarely. Instead, we observe the collection of scalars X_{i1}, \dots, X_{im_i} for $i = 1, \dots, n$ where $\{X_{ij} : j = 1, \dots, m_i\} \sim f_i$. Throughout this paper, we assume that X_{ij} are non-negative continuous random variables and this assumption is very trivial in our data example. For subject i , the function S_i is defined as $1 - F_i(x) = \mathbb{P}\{X_i > x\}$ and is termed the survival function. The survival function represents the probability that a specific event has not occurred by a certain time point x . Here F_i indicates the subject-specific distribution function (DF). Hazard rate (HR) of X_i is defined as $\lambda_i(x) = \lim_{\delta \downarrow 0} \frac{\mathbb{P}\{x < X_i \leq x + \delta | X_i > x\}}{\delta}$ which is the conditional probability that an event will fail the next small interval of time given that the event has been survived at x . If F_i is an absolutely continuous DF with density f_i , the HR for subject i is defined as $(-\infty, \infty)$ by $\lambda_i(x) = f_i(x)/S_i(x)\mathbf{1}\{S_i(x) > 0\} + \infty\mathbf{1}\{S_i(x) = 0\}$ where $\mathbf{1}(x \in A)$ takes value 1 when $x \in A$ and zero otherwise. Moreover, we define the subject-specific quantile function (QF) $Q_i(p) = \inf\{x : F_i(x) \geq p\}$ for $p \in [0, 1]$. In this article, we restrict our attention to the cases where both $F_i(x)$ and $Q_i(p)$ are continuous, which ensures that $Q_i = F_i^{-1}$ satisfying $F_i(Q_i(p)) = p$ and $Q_i(F_i(x)) = x$, which confirms that the QF and DF exhibit strictly ascending behavior within their individual domains.

In addition to the density, survival, hazard, and quantile functions, we also can use the total time on test (TTT) (Epstein & Sobel, 1953; Brunk et al., 1972) function as a choice of the distributional representation. This transformation based on the quantiles was developed in the early 1970s in reliability problems. It has since been applied in other areas such as stochastic modeling, maintenance scheduling, risk assessment, and energy sales. The subject-specific TTT transform of the distribution function F , viz., $T_i(p)$ is defined on the interval $[0, 1]$ as $T_i(p) = \int_0^{Q_i(p)} \{1 - F_i(x)\} dx$. For convenience, we list some of the basic properties below.

- For each i , like quantile function, T_i is defined on $[0, 1]$ which is independent of the subject. By definition, T_i starts from zero, and more importantly, if the mean of the distribution exists, then $Q(1) = \infty$, and as a result, $T_i(1)$ is the mean of the underlying random variable.
- Since we have assumed that the DF is continuous, TTT is an increasing function (moreover the converse is also true).
- TTT is a quantile function and the corresponding distribution is termed as the transformed distribution, $T_i(p) = \psi_i(Q_i(p))$ where $\psi_i(x) = \int_0^x S_i(x) dx$.
- Moreover the baseline DF F_i and QF can uniquely determined by $T_i(p)$.

However, in principle, $\mathbb{E}\{X_i\}$ is a scalar quantity that can be obtained from integrating survival or quantile function over its appropriate range. Therefore, instead of using such a naive summary measure, we would like to consider a function defined on a

closed and bounded interval on \mathbb{R} with the terminal point coinciding with the expectation of the underlying random variable (we assume throughout the expectation exists).

Remark 1. Distributional morphology. The QF can completely characterize the distribution of individual observation. Moreover, the DF determines the TTT and the reverse is also true. In addition, if F_i has hazard rate λ_i then T_i is differentiable and $\frac{\partial T_i(p)}{\partial p}|_{p=F(x)} = \frac{1}{\lambda_i(p)}$. For example, we consider exponentiated Weibull distribution parameterized by scale parameter λ_0 , shape parameter κ_0 and power parameter α_0 with density function

$$f(x; \lambda_0, \kappa_0, \alpha_0) = \frac{\alpha_0 \kappa_0}{\lambda_0} \left\{ \frac{x}{\lambda_0} \right\}^{\kappa_0-1} \{1 - \exp\{-(x/\lambda_0)^{\kappa_0}\}\}^{\alpha_0-1} \exp\{-(x/\lambda_0)^{\kappa_0}\} \mathbf{1}\{x \geq 0\}, \quad (1)$$

where $\lambda_0, \kappa_0, \alpha_0 > 0$ and $\mathbf{1}\{x \in A\}$ is denoted as indicator function that takes value 1 if $x \in A$ and 0 otherwise. We consider the following choices of parameters to demonstrate different shapes of the hazard function. (i) for constant HR $(\lambda_0, \kappa_0, \alpha_0) = (20, 1, 1)$, (ii) for decreasing HR, $(\lambda_0, \kappa_0, \alpha_0) = (5, 0.5, 2)$, (iii) for increasing HR $(\lambda_0, \kappa_0, \alpha_0) = (50, 2, 2)$, (iv) for bathtub-shaped HR $(\lambda_0, \kappa_0, \alpha_0) = (150, 4, 0.15)$ and (v) for unimodal HR $(\lambda_0, \kappa_0, \alpha_0) = (5, 0.55, 4)$. Figure 1 demonstrates the different distributional representations for these parametric families.

To illustrate these five distributional representations for accelerometry data from individuals with MS, Figures 2 (original activity counts) and 3 (log-transformed activity counts) show five distributional representations for two representative subjects: one with a low EDSS score of 1 (minimal disability, shown in blue) and another with a high EDSS score of 6 (greater disability, shown in red). The low EDSS subject exhibits broader distributions, slower declines in survival, and more sustained activity at higher percentiles, indicating greater variability and higher intensity in physical activity. In contrast, the high EDSS subject's curves are more "compressed", with sharper survival declines and hazard peaks at lower activity levels.

3.2 | Estimation of five distributional representations

To pursue statistical modeling with the distributional representations mentioned in Section 3.1, we need to estimate those statistical objects. Here we summarize the estimation procedures of the distribution representations. The density function is estimated by the kernel density estimator as described below.

$$\hat{f}_{i,h_i}(x) = \frac{1}{h_i} \sum_{j=1}^{m_i} K\left(\frac{x - X_{ij}}{h_i}\right), \quad (2)$$

where K is the non-negative kernel function and $h_i > 0$ is a smoothing parameter (a.k.a bandwidth). Under the choice of the Gaussian kernel, the rule of thumb of selecting the subject-specific bandwidth is $h_i \sim 1.06\hat{\sigma}_i m_i^{-1/5}$ where the standard deviation is estimated by X_{i1}, \dots, X_{im_i} (Silverman, 2018). The Kaplan-Meier estimator is used for estimating survival function Kaplan & Meier (1958), given by

$$\hat{S}_i(x) = \prod_{j: X_{ij} \leq x} \left(1 - \frac{D_{ij}}{N_{ij}}\right), \quad (3)$$

where for each subject i , N_{ij} is the number of events occurred after X_{ij} and D_{ij} is the number of events occurred at the interval $[X_{ij-1}, X_{ij})$. Another powerful estimator is Nelson-Aalen estimator (Nelson, 1972; Aalen, 1978) which can produce an estimator for cumulative hazard rate function $\Lambda(x) = \int_0^x \lambda(t)dt = -\log\{S(x)\}$, where $\lambda_i(x) = \lim_{\delta \downarrow 0} \frac{\mathbb{P}\{x \leq X_i < x + \delta | X_i > x\}}{\delta}$. It can be shown that $\hat{\Lambda}_i = \prod_{j: X_{ij} \leq x} \frac{D_{ij}}{N_{ij}}$. At the same time, due to the definition of the integral, $\Lambda_i(x) \approx \sum_{\text{grid points } t \text{ such that } t + \delta} \lambda_i(t)\delta$, by definition of the hazard function, $\lambda_i(x)\delta \approx \mathbb{P}\{x \leq X < x + \delta | X > \delta\}$ could be estimated by D_{ij}/N_{ij} , reasonably. Quantile functions can be estimated by the linear interpolation of the order statistics, which is not required for bandwidth selection in kernel density estimation Parzen (2004). We use the following estimator of quantile functions at level p ,

$$\hat{Q}_i(p) = (1 - \omega)X_{i,[(n+1)p]} + \omega X_{i,[(n+1)p]+1}, \quad (4)$$

where the weight ω satisfies $(n+1)p = [(n+1)p] + \omega$ and $[x]$ denotes the greatest integer that does not greater than x . In most statistical software, tools are readily available to generate estimates of the underlying distributional representations. For instance, in R, the functions `density` and `quantile` from the `stats` package (R Core Team, 2024) are employed to estimate density and quantile functions, while the `survfit` function from the `survival` package (Terry M. Therneau & Patricia M. Grambsch, 2000) is used to estimate survival and hazard functions.

Recall that, the total time on test (TTT) for each subject represents the total time the subject survives from the beginning of the observation period until the event of interest occurs. In other words, in a life-length study involving multiple units, some units will fail while others will survive the test period, and the total time on test statistic is the sum of all observed and incomplete life lengths. When the number of units tested approaches infinity, the limit of this statistic is known as the total time on test transform (Epstein & Sobel, 1953; Brunk et al., 1972). Formally, for subject i , suppose there are m_i items to test and the successive failures are observed at $X_{i,1:m_i} \leq X_{i,2:m_i} \leq \dots \leq X_{i,m_i:m_i}$ are the order statistics from a sample X_{i1}, \dots, X_{im_i} with absolutely continuous DF F_i . Note that the test time observed between 0 and $X_{i,1:m_i}$ is $m_i X_{i,1:m_i}$, that of between $X_{i,1:m_i}$ and $X_{i,2:m_i}$ is $(m_i - 1)(X_{i,2:m_i} - X_{i,1:m_i})$, etc. Therefore, we can calculate the total time on test statistic (TTT-stat) during $(0, x)$, for $x \in (X_{i,r:m_i}, X_{i,r+1:m_i}]$ as

$$\tau_i(x) = m_i X_{i,1:m_i} + (m_i - 1)(X_{i,2:m_i} - X_{i,1:m_i}) + \dots + (m_i - r)(x - X_{i,r:m_i}). \quad (5)$$

It is easy to observe that an estimate of the quantile function $\hat{Q}_i(p) = \inf\{x : \hat{F}_i(x) \geq p\}$, for the empirical distribution function \hat{F}_i

$$\hat{F}_i(x) = \begin{cases} 0, & x \leq X_{i,1:m_i} \\ p_{ij} = j/m_i, & X_{i,j:m_i} < x \leq X_{i,(j+1):m_i} \text{ for } j = 1, \dots, m_i - 1 \\ 1, & x \geq X_{i,m_i:m_i} \end{cases} \quad (6)$$

we have for fixed i ,

$$\lim_{m_i \rightarrow \infty} \lim_{r/m_i \rightarrow p} \tau_i(X_{i,r:m_i})/m_i = \lim_{m_i \rightarrow \infty} \lim_{r/m_i \rightarrow p} \int_0^{\hat{Q}_i(r/m_i)} \{1 - \hat{F}_i(x)\} dx = \int_0^{Q_i(p)} \{1 - F_i(x)\} dx, \quad (7)$$

uniformly in $p \in [0, 1]$. The quantity in the right side of Equation (5) is termed as TTT and denoted by $T_i(p)$.

3.3 | Scalar-on-distribution function regression

Assume Y_i is the subject-specific scalar outcome of interests that could be continuous or discrete from an exponential family. We assume the following scalar-on-functional regression model with distributional representations such as distribution function, and quantile function as predictors.

$$E\{Y_i | X_{i1}, \dots, X_{im_i}\} = \mu_i \text{ where } g(\mu_i) = \alpha + \nu_i \text{ with } \nu_i = \int_0^1 D_i(z) \beta(z) dz. \quad (8)$$

Here $g(\cdot)$ is a known link function and D_i captures the distributional accumulation of X_{i1}, \dots, X_{im_i} as discussed in Section 3.1. The smooth coefficient function $\beta(z)$ represents the functional effect of the transformation of the distribution function at level z . In the growing literature of functional data analysis, there are some available methods for the estimation and for the functional-coefficient in scalar-on-function, for example, see Ramsay & Silverman (2005); Reiss & Ogden (2007); Goldsmith et al. (2011) among many others.

In this article, we follow a smoothing spline estimation technique where we represent the unknown coefficient function $\beta(z)$ in terms of univariate basis functions expansion $\beta(z) = \sum_{k=1}^{\kappa} \theta_k B_k(z)$, where $\{B_k(z)\}_{k=1}^{\kappa}$ is the set of known basis functions over z . In matrix notation, one can write $\beta(z) = \mathbf{B}(z)^T \boldsymbol{\theta}$ where $\mathbf{B}(z) = [B_1(z), \dots, B_{\kappa}(z)]^T$ is the vector of known basis function and $\boldsymbol{\theta} = (\theta_1, \dots, \theta_{\kappa})^T$ is the vector of unknown coefficients. In this article, we have used B-spline due to its practicability De Boor et al. (1978). Therefore, the linear functional effect can be re-written as $\int D_i(z) \beta(z) dz = \sum_{k=1}^{\kappa} \theta_k \int D_i(z) B_k(z) dz = \sum_{k=1}^{\kappa} \theta_k W_{ik} = \mathbf{W}_i^T \boldsymbol{\theta}$ where $W_{ik} = \{\int_0^1 D_i(z) B_k(z) dz\}$ and $\mathbf{W}_i = (\mathbf{W}_{i1}, \dots, \mathbf{W}_{i\kappa})^T$.

Thus, from the above discussion, we can rewrite Equation (8) as $g(\mu_i) = \alpha + \mathbf{W}_i^T \boldsymbol{\theta}$ where the unknown is $\alpha, \boldsymbol{\theta}$, to estimate them, use the penalized log-likelihood criterion as following.

$$\mathcal{R}(\alpha, \beta(\cdot)) = -2 \log \mathcal{L}(\alpha, \boldsymbol{\theta}; Y_i, \mathbf{W}_i) + \mathcal{P}(\boldsymbol{\theta}) \quad (9)$$

where \mathcal{P} is the penalty based on the smoothness of the coefficient function. We define $\mathcal{P} = \lambda \int \{\beta''(z)\}^2 dz = \lambda \boldsymbol{\theta}^T \mathbb{P} \boldsymbol{\theta}$ where β'' denotes the second derivative of the smooth function β and the penalty matrix \mathbb{P} is given by $\mathbb{P} = \int \boldsymbol{\theta}''(z)^T \boldsymbol{\theta}''(z) dz$. Therefore, we implement the minimization of \mathcal{R} using the Newton-Raphson method under the generalized additive models Wood et al. (2016); Wood (2017). The smoothing parameter λ is chosen using REML, information criteria such as AIC, BIC, or data-driven

techniques such as generalized cross-validation. For implementation using popular statistical software R R Core Team (2023), we use `refund` package Goldsmith et al. (2020).

Remark 2. Rationale behind using TTT. Numerous alternatives exist for the selection of D_i , encompassing options like DF or QF Ghosal et al. (2021). Given such an array of possibilities, when $\beta(p) = \beta$ holds as a constant, the relationship $\nu_i = \beta \int_0^1 D_i(p)dp = \beta \mathbb{E}\{X_i\}$ becomes apparent. This, in turn, leads to the simplification of the model described in Equation (8) into the conventional generalized linear model with scalar predictors and responses. Consequently, the consideration of the distributional aggregation of X_{ij} s is overlooked, resulting in a compromise of predictive performance. Moreover, due to the mathematical properties of total time on the test, $T_i(1)$ is the same as the mean of the underlying distribution, viz., $\nu_i = \beta \times T_i(1)$. Rather than focusing solely on the endpoint of a function, a more insightful approach involves incorporating the complete function as a predictor within Model (8). This can be achieved through a generalized form of $\nu_i = \int_0^1 \beta(p)T_i(p)dp$, offering a broader perspective for prediction.

4 | APPLICATION TO HEAL-MS STUDY

In this section, we present detailed analyses of the accelerometry data from the HEAL-MS study to compare the discriminatory performance of five distributional representations. We model two outcomes: (i) disability as a binary variable (low vs. high EDSS) and (ii) original EDSS scores. In both cases, we use all five distributional representations and scalar average activity counts within 8am-8pm time interval, obtained using both original and log-transformed activity counts.

We estimated quantile and TTT functions over percentile levels, while density, survival, and hazard functions are approximated across the entire range of minute-level activity counts. Figures 4 and 5 show the scalar and distributional summaries of activity counts on both original and log-transformed scales, respectively. Bold solid lines represent the simple point-wise averages of the distributional representations for different groups. It is important to note that some of these representations serve primarily as point-wise summaries and may not convey deeper statistical meaning and a proper distributional representation.

To assess the discriminatory performance of the six predictors, we utilize cross-validated Area Under the Curve (cvAUC) for the binary and cvR^2 for the continuous outcome, respectively. To ensure the reliability of our validation, we employ a rigorous 5-fold cross-validation technique with 100 random replications and present the average cross-validated AUC and cross-validated R^2 along with corresponding 95% confidence intervals to provide a comprehensive understanding of the model's performance in Table 1.

Figures 6 and 7 show estimated regression coefficient functions obtained from the distributional scalar-on-function logistic regression models. Similarly, Figures 8 and 9 show estimated regression coefficient functions obtained from the distributional scalar-on-function Gaussian regression models for predicting the EDSS where all distributional representations are calculated based on the original and log-transformed activity counts, respectively.

Key findings are summarized as follows:

Binary disability (High vs. Low EDSS):

- * The hazard function demonstrated the highest discriminatory power, with a cvAUC of 0.77 (95% CI: 0.76–0.78) when using original activity counts and 0.77 (95% CI: 0.76–0.78) with log-transformed counts.
- * The quantile function provided the second-highest performance, achieving a cvAUC of 0.76 (95% CI: 0.74–0.77). Conventional scalar summaries showed significantly lower performance, with cvAUCs of 0.70 (95% CI: 0.69–0.71) and 0.65 (95% CI: 0.64–0.66) for original and log-transformed counts, respectively.

Continuous disability (original EDSS scores):

- * The hazard function again demonstrated superior performance, achieving an cvR^2 of 0.26 (95% CI: 0.23–0.28) for original counts and 0.25 (95% CI: 0.24–0.27) for log-transformed counts.
- * The quantile and TTT functions showed comparable performance, with cvR^2 values ranging in 0.23–0.24. Scalar summaries performed poorly, with cvR^2 values of 0.13 (original AC) and 0.1 (log-transformed AC).

Additional observations are as follows.

- Modeling MS status based on activity counts (AC): From the output of the classical logistic regression, we find that the subject-specific average PA is significantly associated (with the level of significance $\alpha = 0.05$) with lower log odds of MS, $\hat{\beta}_{AC[8am-8pm]} = -0.001$ (0.0002). Figure 6 further illustrates the distribution effects of log-odds of MS based on AC.
- Modeling MS status based on log-activity counts (LAC): Using the classical logistic regression, we find the subject-specific average PA is significantly associated with lower log odds of MS $\hat{\beta}_{AC[8am-8pm]} = -0.65$ (0.11). Figure 7 illustrates the distribution effects of log-odds of MS based on LAC. Statistically, both the quantile and TTT function are significantly associated with lower odds of MS, survival of higher LAC is significantly associated with lower odds of MS, and survival of higher LAC is significantly associated with higher odds of MS.
- Modeling EDSS score based on AC: Based on the classical regression model, we obtain subject-specific average PA is significantly associated with EDSS $\hat{\beta}_{AC[8am-8pm]} = -0.001$ (0.0001). In figure 8, we demonstrate the distributional effect of EDSS based on AC. The effect of the density function is significantly associated with lower EDSS, hazard for lower PA is significantly associated with lower EDSS. Higher levels of quantile and TTT functions are associated with lower EDSS.
- Modeling EDSS score based on LAC: Based on the classical regression model, we obtain subject-specific average PA is significantly associated with EDSS $\hat{\beta}_{AC[8am-8pm]} = -0.51$ (0.11). In figure 9, we demonstrate the distributional effect of EDSS based on log-transformed AC. The effect of survival for higher PA is significantly associated with lower EDSS. Similar to the previous situation, higher levels of quantile and TTT functions are associated with lower EDSS.

Based on the outcome of the fitted model, we are also interested in calculating the regression biomarkers and comparing them across distributional representations. The biomarkers based on the models with density, survival, hazard, quantile, TTT functions, and average physical activity as covariates are defined as follows. (i) $DBM_{f,i} = \int f_i(x) \hat{\beta}_f(x) dx$, (2) $DBM_{S,i} = \int S_i(x) \hat{\beta}_S(x) dx$, (3) $DBM_{\lambda,i} = \int \lambda_i(x) \hat{\beta}_\lambda(x) dx$, (4) $DBM_{Q,i} = \int Q_i(p) \hat{\beta}_Q(p) dp$, (5) $DBM_{TTT,i} = \int T_i(p) \hat{\beta}_T(x) dp$ and (6) $BM_{a,i} = \overline{AC}_i \hat{\beta}_{AC,i[8am-8pm]}$. Figures 10, 11 demonstrate the scatter-plot matrices for all five types of biomarkers to discriminate the MS status where the distributional and scalar summaries are obtained from counts in original and log scale, respectively. In addition, similar to the earlier case, Figures 12 and 13 display the scatter-plot matrices for all five biomarkers to discriminate the EDSS where the distributional and scalar summaries are obtained from counts in original and log scale, respectively. We can clearly see that the biomarkers fall into three distinct groups based on their cross-correlations. Density and CDF-based biomarkers are very similar between each other and are highly correlated with the average activity counts. On the other hand, quantile and TTT-based biomarkers are highly correlated, capturing very similar information across quantile levels. *Hazard-based biomarkers stand out by uniquely capturing tail information not captured by the other four unconditional distributional representations.*

5 | DISCUSSION

In this paper, we compared five individual-specific distributional representations to capture distributional information in the physical activity assessed by accelerometry. We developed scalar-on-function regression models using the proposed distributional representations, including unconditional probability-based domains and quantile domains. We demonstrate the benefits of modeling the distributional aspect of accelerometry data that significantly increased the power to discriminate disability levels in individuals with MS. Among the distributional representations explored in the HEAL-MS study, the hazard function demonstrated the highest discriminatory power.

From a clinical perspective, more sensitive distributional representation aggregating daily activity can help accelerate the conduct of clinical trials of candidate neuroprotective medications. This is important since the approved medications for MS do not appear to work in the progressive phase of the illness in the absence of ongoing attacks on myelin.

From a mathematical perspective, all five distributional representations could be re-expressed in terms of each other. However, from a predictive modeling perspective, we are often interested in using linear functional models. This may favor certain distributional representations, as illustrated in our exploratory case study.

This research highlights the value of distributional information as a novel highly sensitive biomarker and endpoint in clinical studies, offering a more accurate way to capture within-subject variability in accelerometry data. Our group will apply these endpoints to track the longitudinal change in disability of the participants of the HEAL-MS study. Similar approaches can be used in data generated by other sDHT modalities including continuous glucose monitoring and heart rate monitors. In future work, we plan to incorporate temporal and longitudinal information in the characterization of distributions.

ACKNOWLEDGEMENTS

This research was partially supported by the grant R01NR018851 from the National Institute of Health (NIH).

FINANCIAL DISCLOSURE

EM disclosed research support from Biogen, Roche/Genentech. Consulting fees from BeCareLink, LLC. Royalties for editorial duties from UpToDate.

CONFLICT OF INTERESTS

The authors declare no potential conflicts of interests

REFERENCES

- Aalen, O. (1978). Nonparametric inference for a family of counting processes. *The Annals of Statistics*, 701–726.
- Abbadessa, G., Lavorgna, L., Miele, G., Mignone, A., Signoriello, E., Lus, G., ... Bonavita, S. (2021). Assessment of multiple sclerosis disability progression using a wearable biosensor: a pilot study. *Journal of Clinical Medicine*, 10(6), 1160.
- Augustin, N. H., Mattocks, C., Faraway, J. J., Greven, S., & Ness, A. R. (2017). Modelling a response as a function of high-frequency count data: the association between physical activity and fat mass. *Statistical methods in medical research*, 26(5), 2210–2226.
- Brunk, H., Barlow, R. E., Bartholomew, D. J., & Bremner, J. M. (1972). Statistical inference under order restrictions.(the theory and application of isotonic regression). *International Statistical Review*, 41, 395.
- Chen, Y., Lin, Z., & Müller, H.-G. (2021). Wasserstein regression. *Journal of the American Statistical Association*, 1–14.
- De Boor, C., De Boor, C., Mathématicien, E.-U., De Boor, C., & De Boor, C. (1978). *A practical guide to splines* (Vol. 27). springer-verlag New York.
- Epstein, B., & Sobel, M. (1953). Life testing. *Journal of the American Statistical Association*, 48(263), 486–502.
- Ezeugwu, V., Klaren, R. E., Hubbard, E. A., Manns, P. T., & Motl, R. W. (2015). Mobility disability and the pattern of accelerometer-derived sedentary and physical activity behaviors in people with multiple sclerosis. *Preventive medicine reports*, 2, 241–246.
- Fang, Z., Guo, Z.-C., & Zhou, D.-X. (2020). Optimal learning rates for distribution regression. *Journal of complexity*, 56, 101426.
- Ghodrati, L., & Panaretos, V. M. (2022). Distribution-on-distribution regression via optimal transport maps. *Biometrika*, 109(4), 957–974.
- Ghosal, R., Varma, V., Volfson, D., Hillel, I., Urbanek, J., Hausdorff, J., ... Zipunnikov, V. (2021). Distributional data analysis via quantile functions and its application to modeling digital biomarkers of gait in alzheimer's disease. *Biostatistics (Oxford, England)*, kxab041–kxab041.
- Goldsmith, J., Bobb, J., Crainiceanu, C. M., Caffo, B., & Reich, D. (2011). Penalized functional regression. *Journal of computational and graphical statistics*, 20(4), 830–851.
- Goldsmith, J., Scheipl, F., Huang, L., Wrobel, J., Di, C., Gellar, J., ... Reiss, P. T. (2020). refund: Regression with functional data [Computer software manual]. Retrieved from <https://CRAN.R-project.org/package=refund> R package version 0.1-23.
- Hron, K., Menafoglio, A., Templ, M., Hruzova, K., & Filzmoser, P. (2016). Simplicial principal component analysis for density functions in bayes spaces. *Computational Statistics & Data Analysis*, 94, 330–350.
- Kaplan, E. L., & Meier, P. (1958). Nonparametric estimation from incomplete observations. *Journal of the American statistical association*, 53(282), 457–481.
- Keller, J. L., Tian, F., Fitzgerald, K. C., Mische, L., Ritter, J., Costello, M. G., ... Zackowski, K. M. (2022). Using real-world accelerometry-derived diurnal patterns of physical activity to evaluate disability in multiple sclerosis. *Journal of Rehabilitation and Assistive Technologies Engineering*, 9, 20556683211067362.
- Leroux, A., Di, J., Smirnova, E., McGuffey, E. J., Cao, Q., Bayatmokhtari, E., ... Crainiceanu, C. (2019). Organizing and analyzing the activity data in nhanes. *Statistics in biosciences*, 11, 262–287.

- Marshall, A. W., & Olkin, I. (2007). *Life distributions* (Vol. 13). Springer.
- Matabuena, M., & Petersen, A. (2021). Distributional data analysis of accelerometer data from the nhanes database using nonparametric survey regression models. *arXiv preprint arXiv:2104.01165*.
- Matabuena, M., Petersen, A., Vidal, J. C., & Gude, F. (2021). Glucodensities: a new representation of glucose profiles using distributional data analysis. *Statistical methods in medical research*, 30(6), 1445–1464.
- Nair, N. U., Sankaran, P., & Balakrishnan, N. (2013). *Quantile-based reliability analysis*. Springer Science & Business Media.
- Nelson, W. (1972). Theory and applications of hazard plotting for censored failure data. *Technometrics*, 14(4), 945–966.
- Oliva, J., Póczos, B., & Schneider, J. (2013). Distribution to distribution regression. In *International conference on machine learning* (pp. 1049–1057).
- Parzen, E. (2004). Quantile probability and statistical data modeling. *Statistical Science*, 652–662.
- Petersen, A., & Müller, H.-G. (2016). Functional data analysis for density functions by transformation to a hilbert space. *The Annals of Statistics*, 183–218.
- Petersen, A., & Müller, H.-G. (2019). Fréchet regression for random objects with euclidean predictors. *The Annals of Statistics*, 47(2), 691–719.
- Petersen, A., Zhang, C., & Kokoszka, P. (2022). Modeling probability density functions as data objects. *Econometrics and Statistics*, 21, 159–178.
- Póczos, B., Singh, A., Rinaldo, A., & Wasserman, L. (2013). Distribution-free distribution regression. In *Artificial intelligence and statistics* (pp. 507–515).
- R Core Team. (2023). R: A language and environment for statistical computing [Computer software manual]. Vienna, Austria. Retrieved from <https://www.R-project.org/>
- R Core Team. (2024). R: A language and environment for statistical computing [Computer software manual]. Vienna, Austria. Retrieved from <https://www.R-project.org/>
- Ramsay, J. O., & Silverman, B. W. (2005). *Functional data analysis*. Springer series in statistics.
- Reiss, P. T., & Ogden, R. T. (2007). Functional principal component regression and functional partial least squares. *Journal of the American Statistical Association*, 102(479), 984–996.
- Rjeily, N. B., Hu, C., Dewey, B., Hulett, C., Dagher, G., Lee, A. Z., ... others (2022). Using actigraphy to track clinical disability progression in multiple sclerosis: Baseline analysis of the heal-ms study. In *Multiple sclerosis journal* (Vol. 28, pp. 61–62).
- Silverman, B. W. (2018). *Density estimation for statistics and data analysis*. Routledge.
- Smirnova, E., Leroux, A., Cao, Q., Tabacu, L., Zipunnikov, V., Crainiceanu, C., & Urbanek, J. K. (2020). The predictive performance of objective measures of physical activity derived from accelerometry data for 5-year all-cause mortality in older adults: National health and nutritional examination survey 2003–2006. *The Journals of Gerontology: Series A*, 75(9), 1779–1785.
- Szabó, Z., Sriperumbudur, B. K., Póczos, B., & Gretton, A. (2016). Learning theory for distribution regression. *The Journal of Machine Learning Research*, 17(1), 5272–5311.
- Talská, R., Hron, K., & Grygar, T. M. (2021). Compositional scalar-on-function regression with application to sediment particle size distributions. *Mathematical Geosciences*, 53(7), 1667–1695.
- Terry M. Therneau, & Patricia M. Grambsch. (2000). *Modeling survival data: Extending the Cox model*. New York: Springer.
- Tian, F., Fitzgerald, K., Keller, J., Zackowski, K., Zipunnikov, V., & Mowry, E. (2020). A longitudinal study of objectively-measured physical activity patterns in multiple sclerosis. In *Multiple sclerosis journal* (Vol. 26, pp. 25–25).
- Wood, S. N. (2017). *Generalized additive models: an introduction with r*. CRC press.
- Wood, S. N., Pya, N., & Säfken, B. (2016). Smoothing parameter and model selection for general smooth models. *Journal of the American Statistical Association*, 111(516), 1548–1563.
- Yang, H., Baladandayuthapani, V., Rao, A. U., & Morris, J. S. (2020). Quantile function on scalar regression analysis for distributional data. *Journal of the American Statistical Association*, 115(529), 90–106.

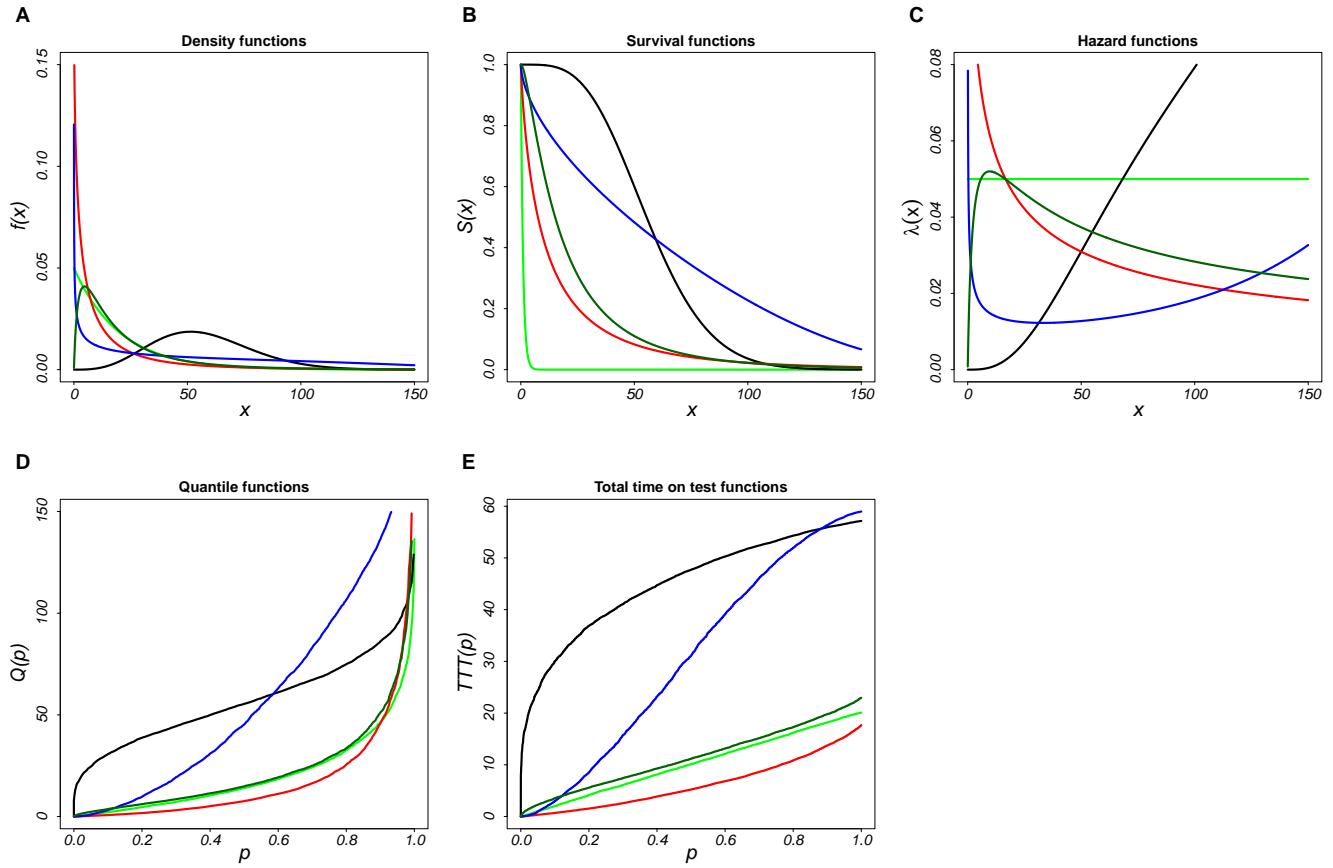


FIGURE 1 Distributional morphology: Density functions (A), survival functions (B), hazard functions (C) with corresponding quantile functions (D), and corresponding TTT functions (E). Here the underlying distribution is an exponentiated Weibull distribution and we consider the different scale, shape, and power parameters so that we obtain the different shapes of the hazard functions.

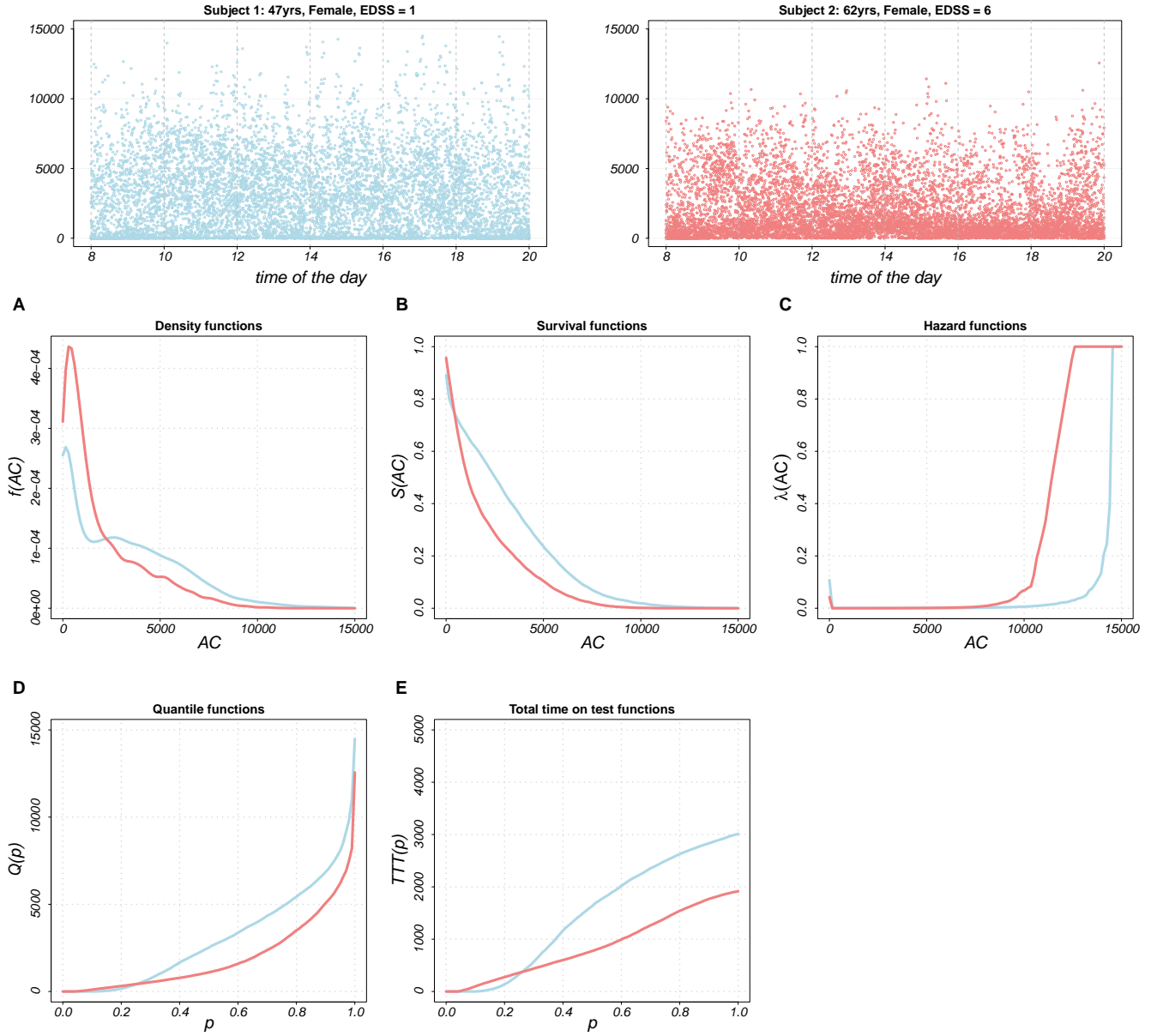


FIGURE 2 Five distributional summaries of activity counts (AC) for two subjects: Density functions (A), survival functions (B), hazard functions (C) with corresponding quantile functions (D), and corresponding TTT functions (E).

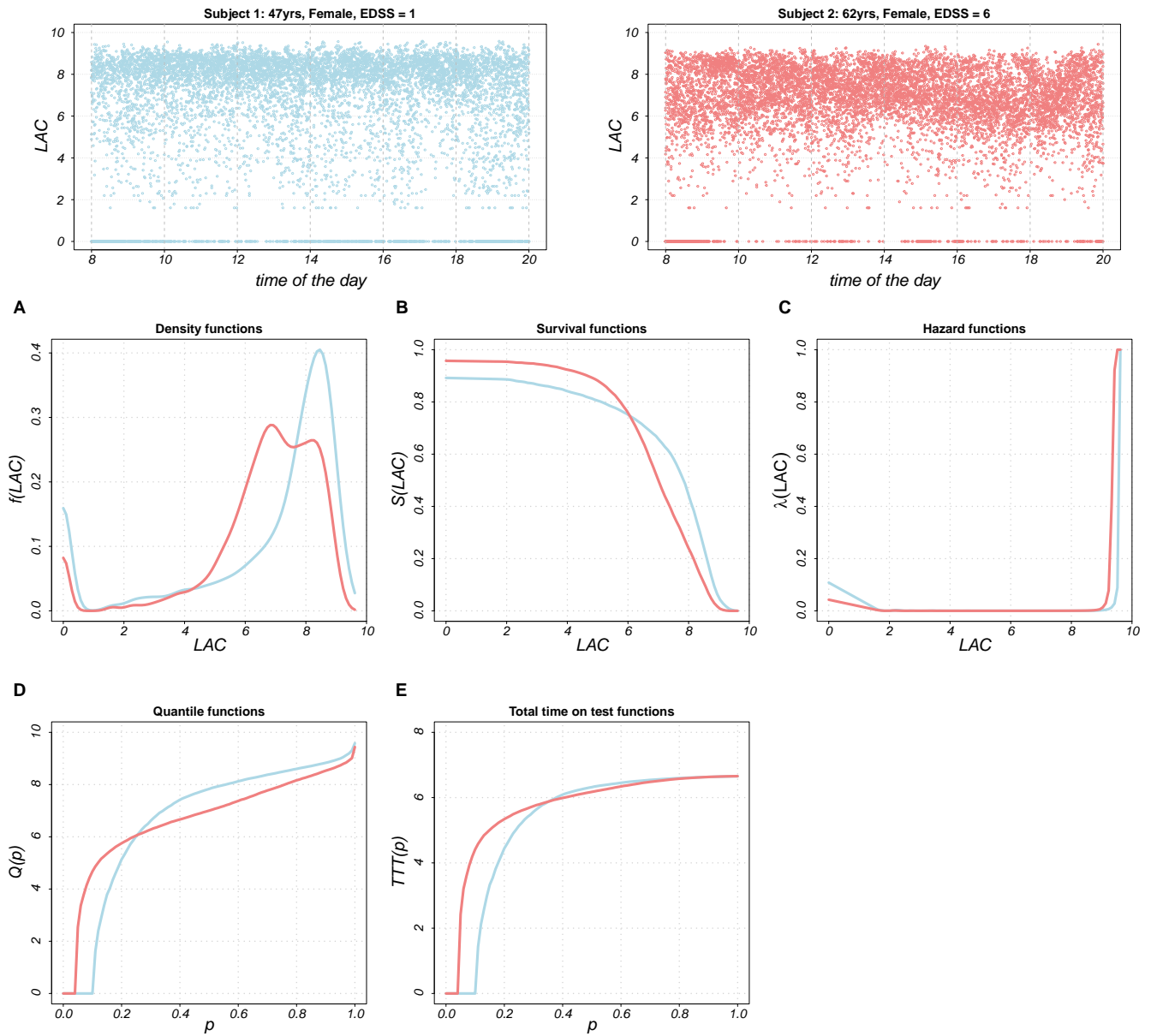


FIGURE 3 Five distributional summaries of log-transformed activity counts (LAC) for two subjects: Density functions (A), survival functions (B), hazard functions (C) with corresponding quantile functions (D), and corresponding TTT functions (E).

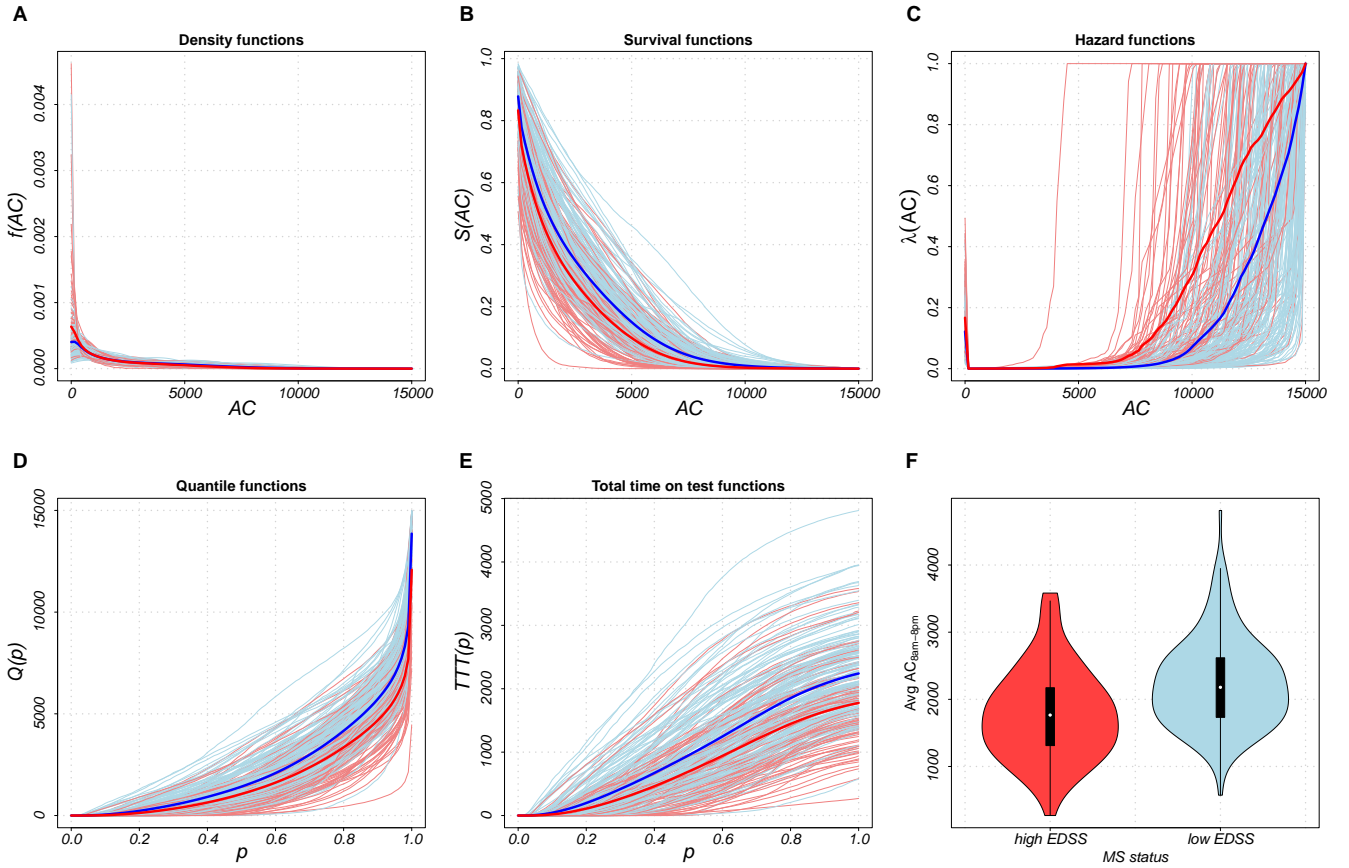


FIGURE 4 Distributional and scalar summaries of activity counts (AC): Density functions (A), survival functions (B), hazard functions (C) with corresponding quantile functions (D), and corresponding TTT functions (E). In addition, the violin-plot of scalar summaries is also shown in (F). Two MS statuses based on EDSS (high vs low) are color-coded by light red and blue, respectively. The solid red and blue lines indicate the barycenter of the corresponding distributional representations for MS classes with low and high EDSS, respectively.

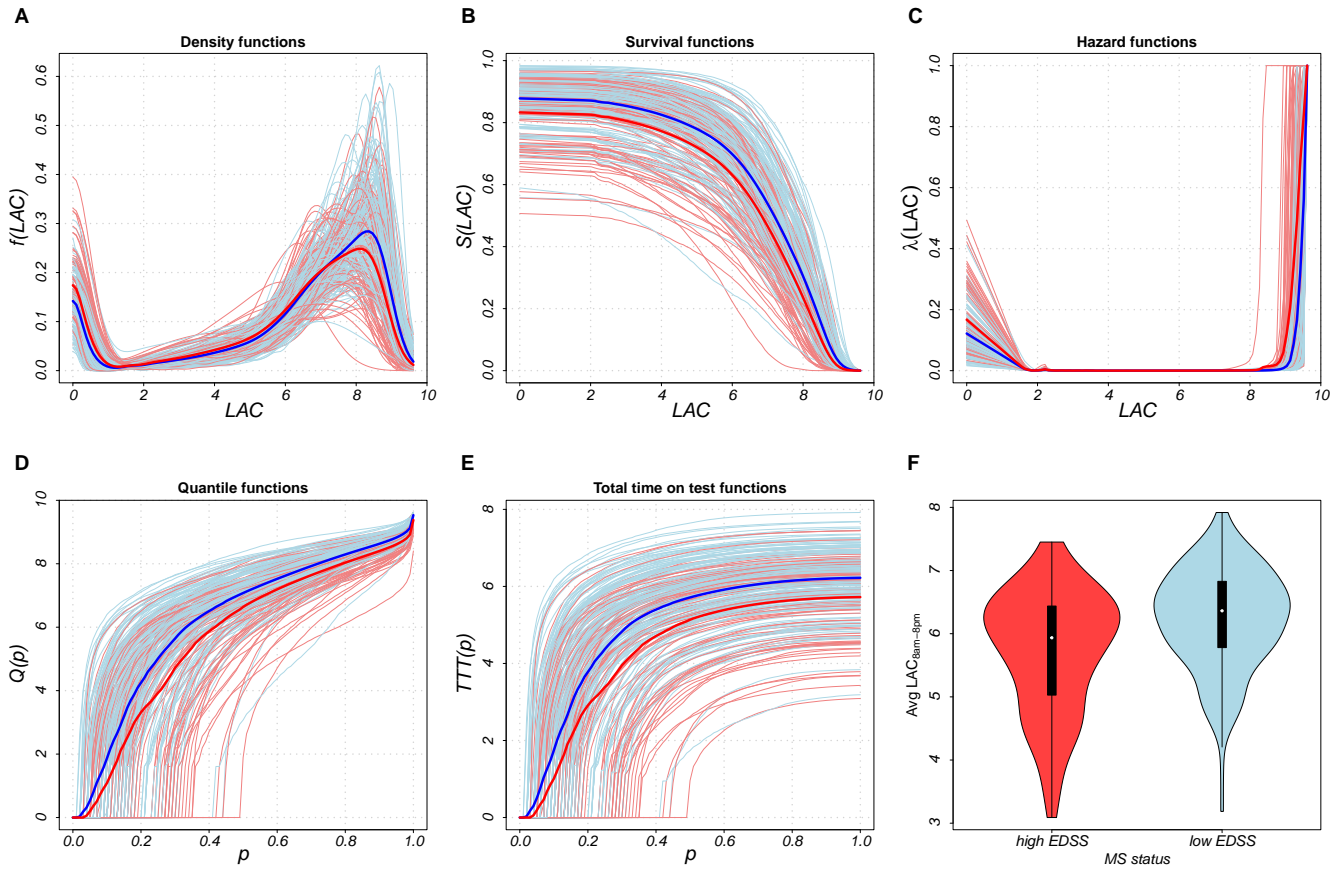


FIGURE 5 Distributional and scalar summaries of log activity counts (LAC): Density functions (A), survival functions (B), hazard functions (C) with corresponding quantile functions (D), and corresponding TTT functions (E). In addition, the violin-plot of scalar summaries is also shown in (F). Two MS statuses based on EDSS (high vs low) are color-coded by light red and blue, respectively. The solid red and blue lines indicate the barycenter of the corresponding distributional representations for MS classes with low and high EDSS, respectively.

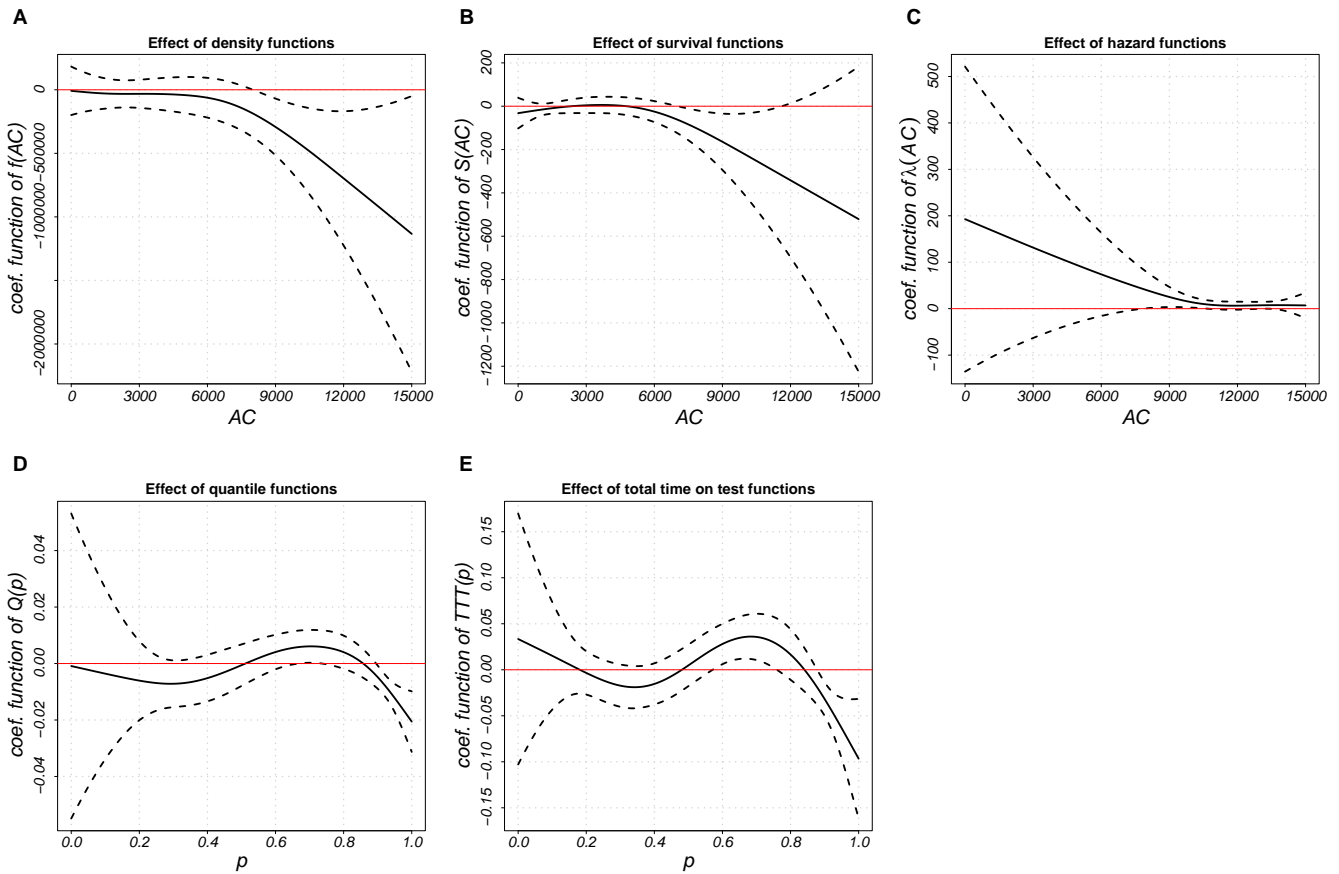


FIGURE 6 The estimated regression coefficients for the models with different distributional representations were obtained from scalar-on-function *logistic regressions to model MS status*, where the distributional and scalar summaries are obtained based on *activity counts*. A solid black curve indicates the estimated coefficient function, dotted black lines indicate 95% confidence intervals.

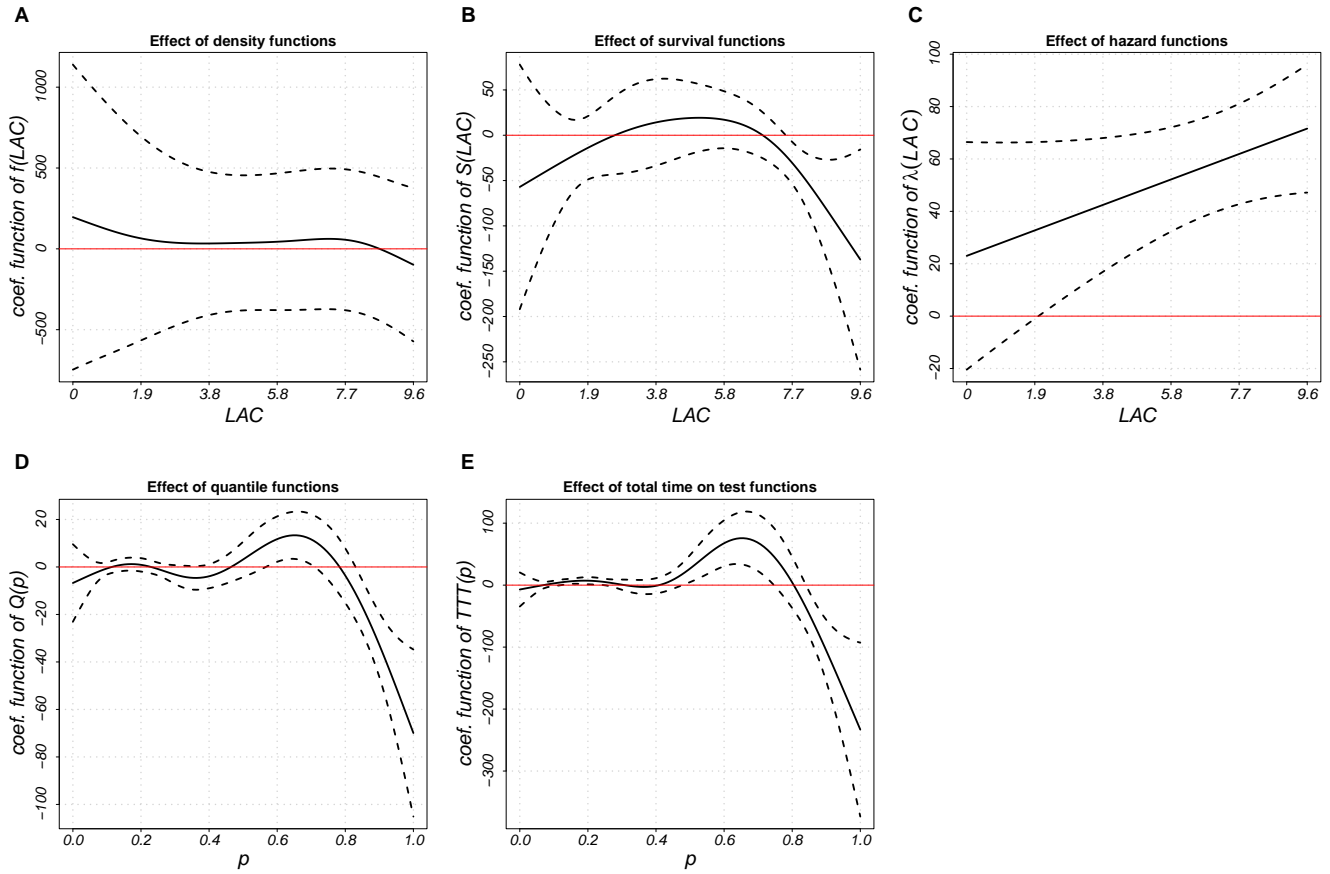


FIGURE 7 The estimated regression coefficients for the models with different distributional representations were obtained from *scalar-on-function logistic regressions to model MS status*, where the distributional and scalar summaries are obtained based on *log-activity counts*. A solid black curve indicates the estimated coefficient function, dotted black lines indicate 95% confidence intervals.

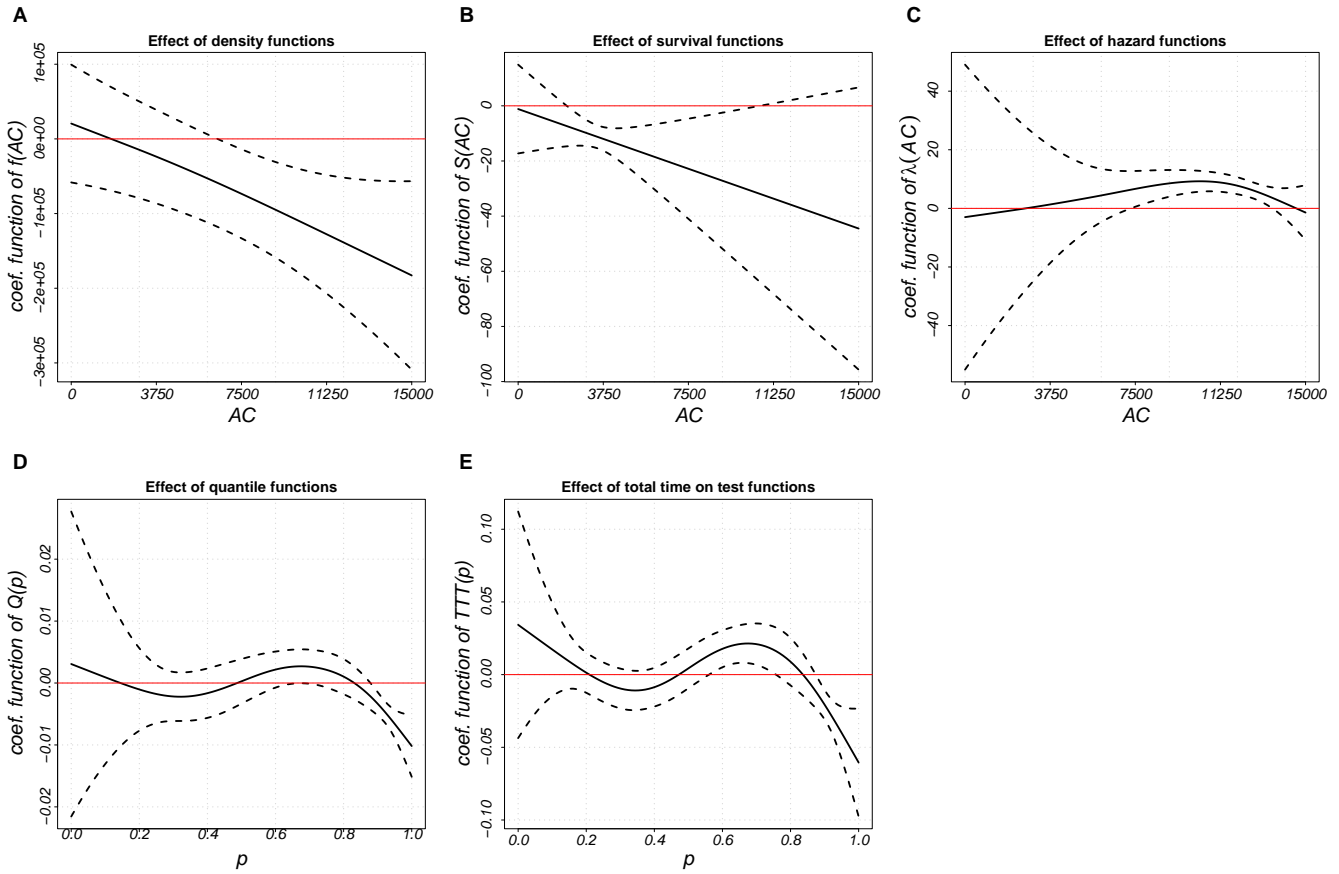


FIGURE 8 The estimated regression coefficients for the models with different distributional representations were obtained from *scalar-on-function regressions to model EDSS scores*, where the distributional and scalar summaries are obtained based on *activity counts*. A solid black curve indicates the estimated coefficient function, dotted black lines indicate 95% confidence intervals.

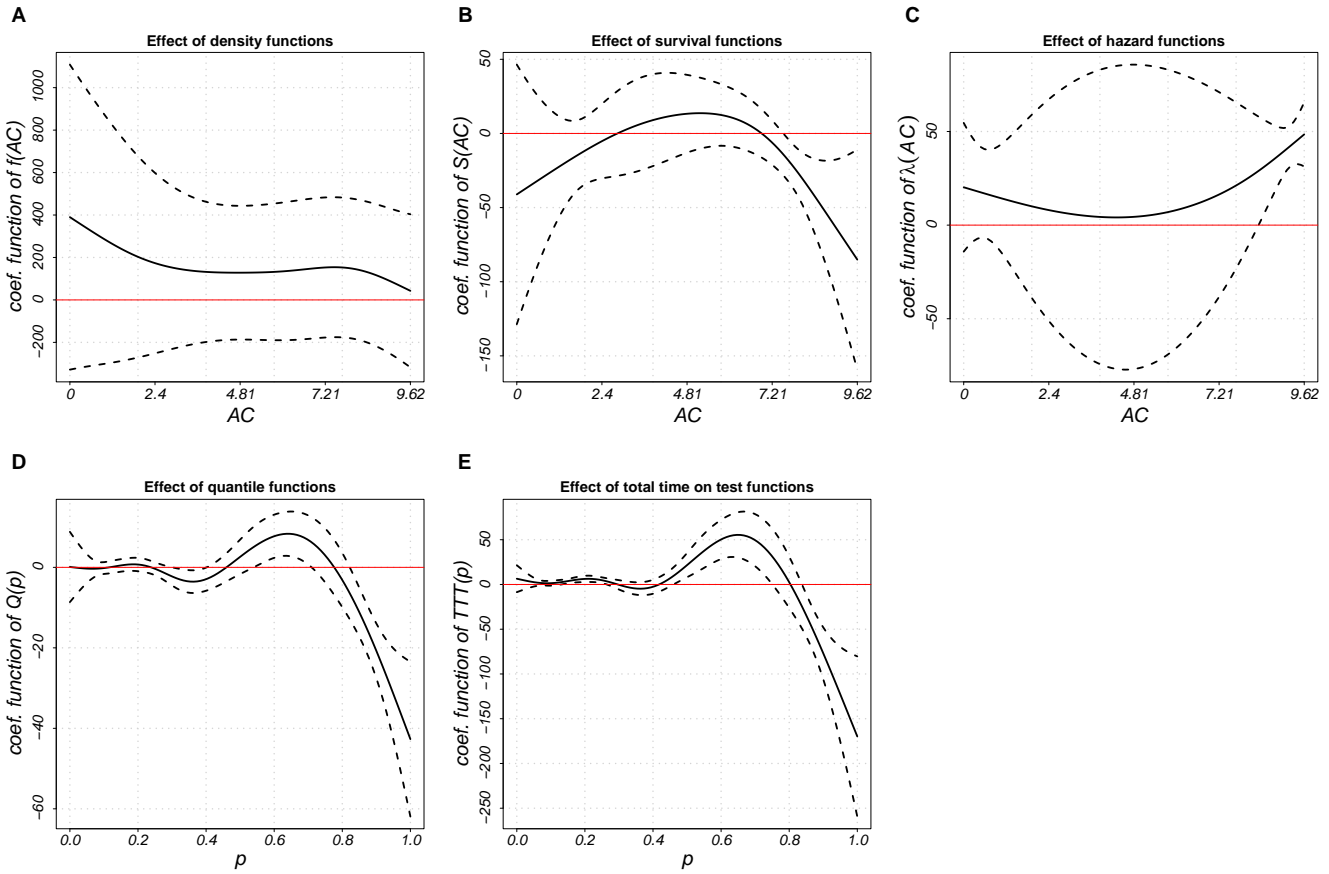


FIGURE 9 The estimated regression coefficients for the models with different distributional representations were obtained from *scalar-on-function regressions to model EDSS scores*, where the distributional and scalar summaries are obtained based on *log-activity counts*. A solid black curve indicates the estimated coefficient function, dotted black lines indicate 95% confidence intervals.

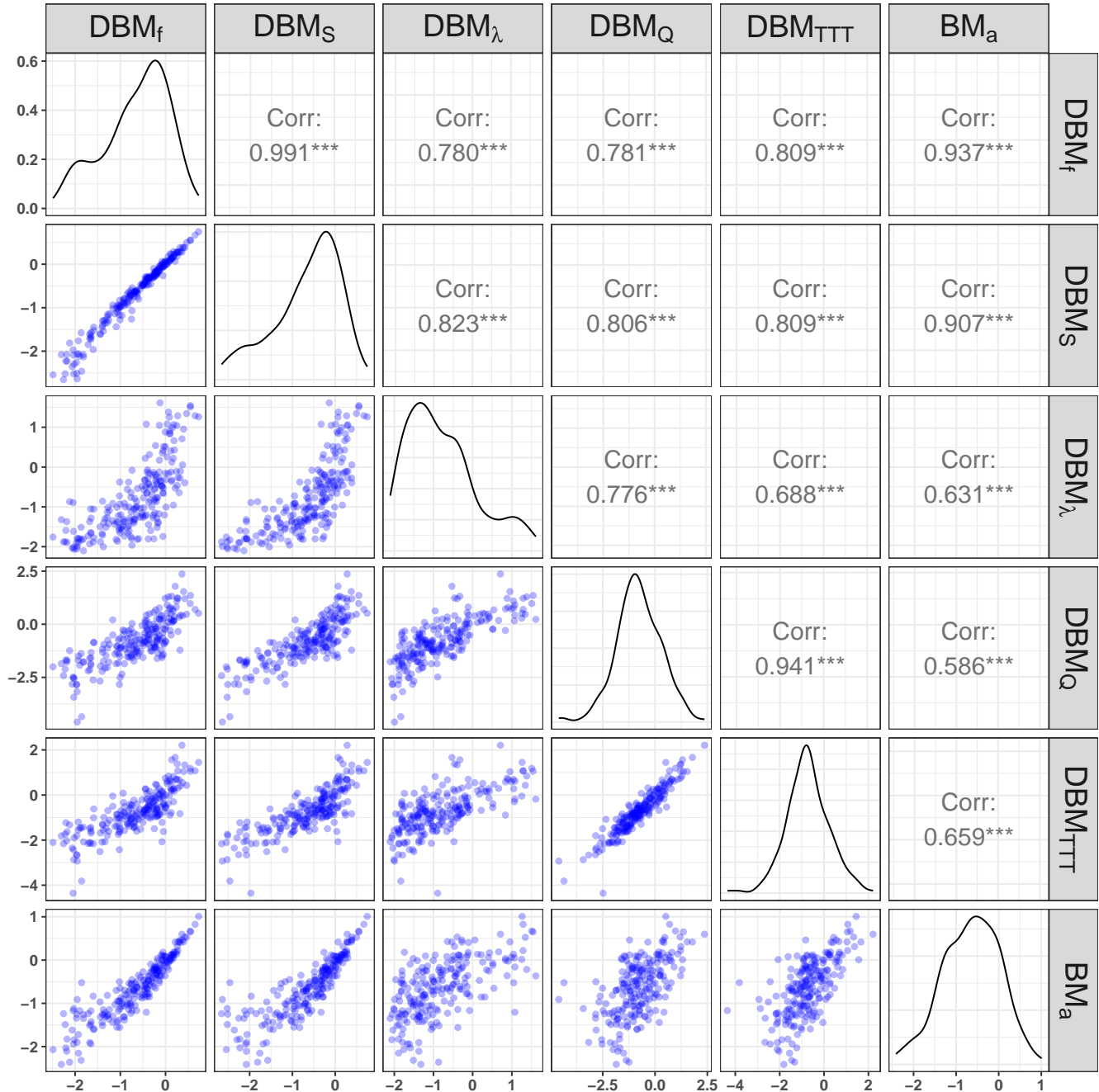


FIGURE 10 Scatter plots of the estimated weighted scores corresponding to the covariates density, survival, hazard, quantile, and TTT functions along with the average physical activity counts to *predict the MS status*, where the distributional and scalar summaries are obtained based on *activity counts*. The upper triangular entries indicate the Spearman's correlation coefficients between the associated row and columns.

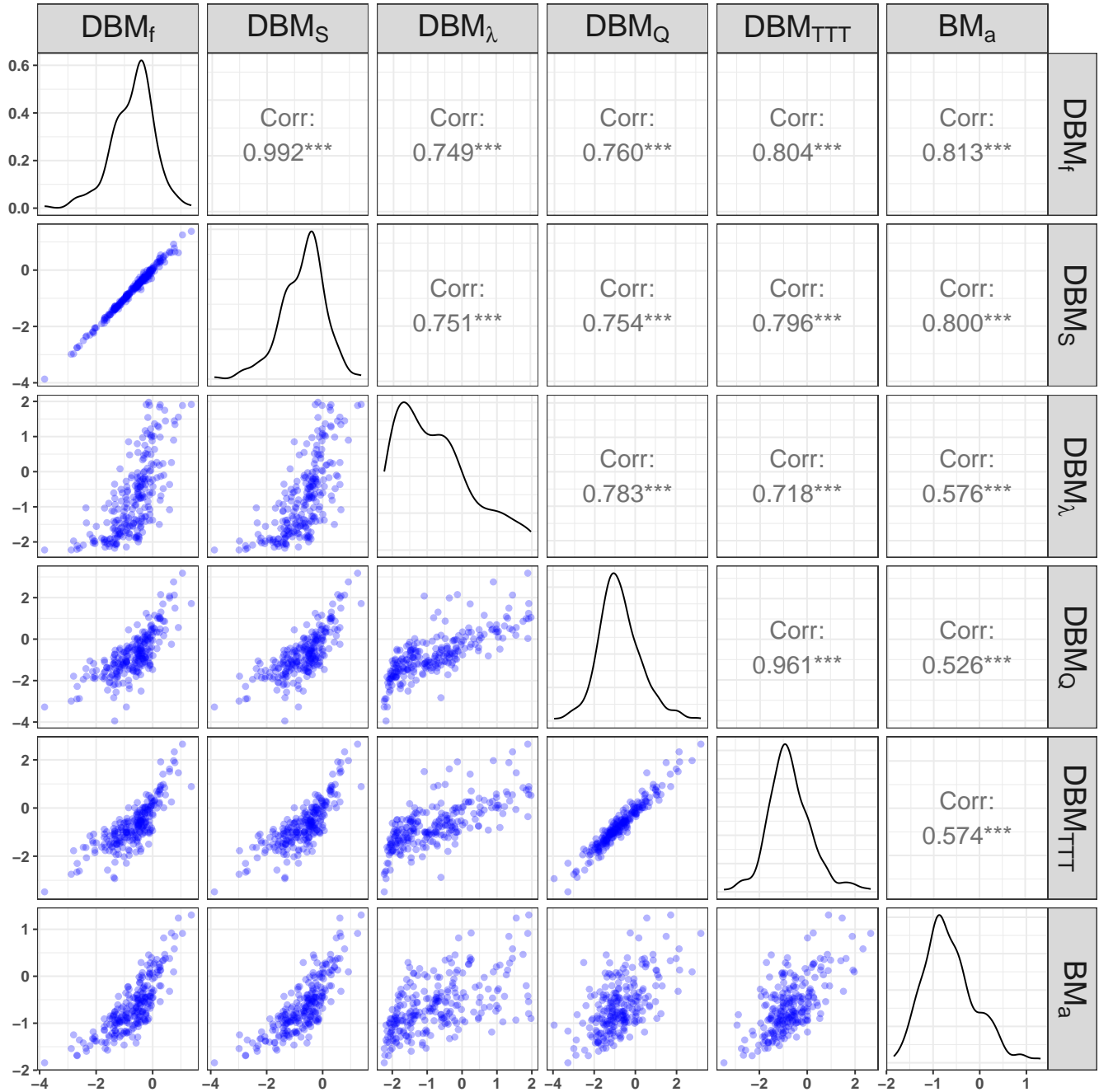


FIGURE 11 Scatter plots of the estimated weighted scores corresponding to the covariates density, survival, hazard, quantile, and TTT functions along with the average physical activity counts to *predict the EDSS scores*, where the distributional and scalar summaries are obtained based on *log-activity counts*. The upper triangular entries indicate the Spearman's correlation coefficients between the associated row and columns.

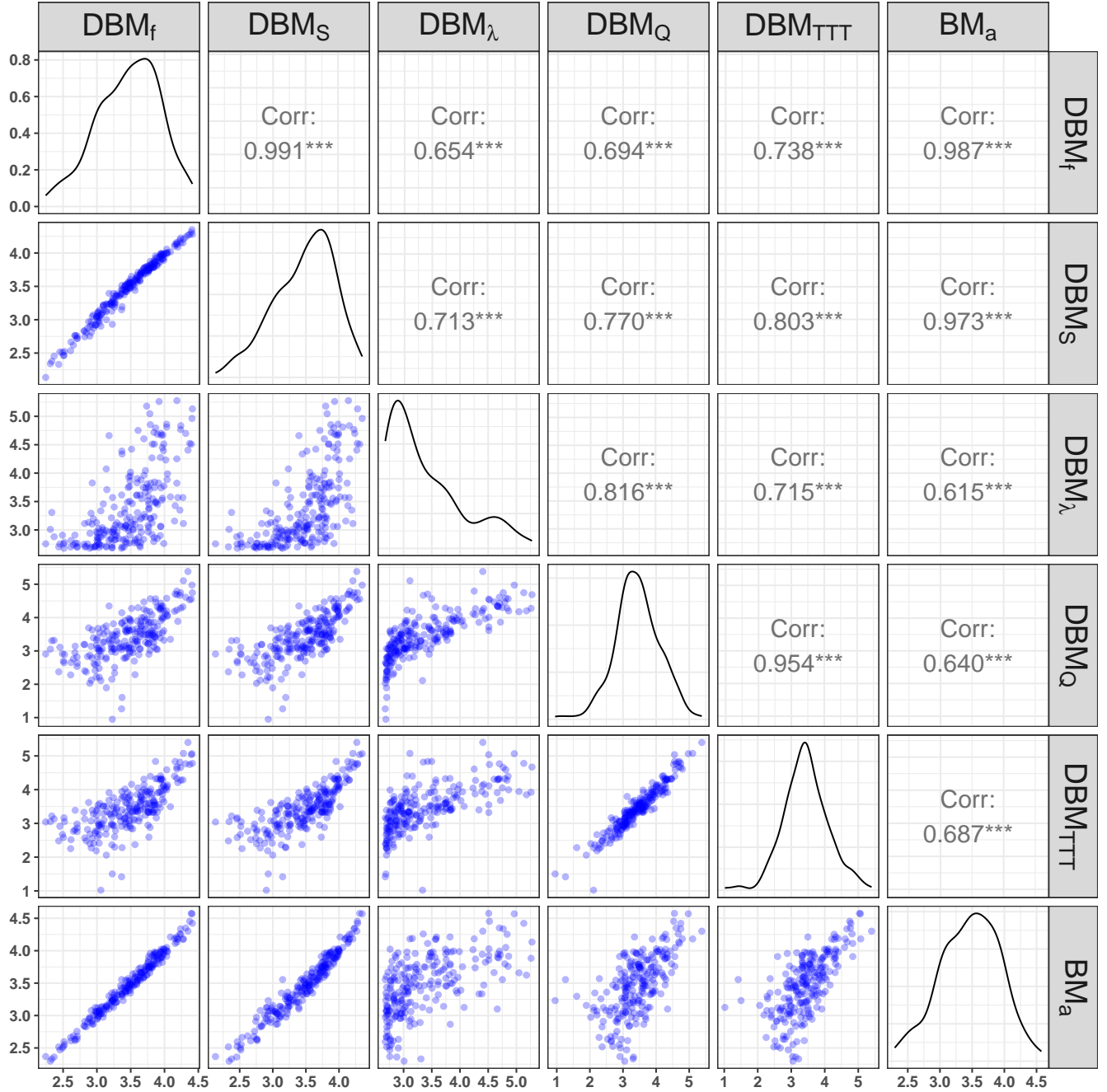


FIGURE 12 Scatter plots of the estimated weighted scores corresponding to the covariates density, survival, hazard, quantile, and TTT functions along with the average physical activity counts to *predict EDSS scores*, where the distributional and scalar summaries are obtained based on *activity counts*. The upper triangular entries indicate the Spearman's correlation coefficients between the associated row and columns.

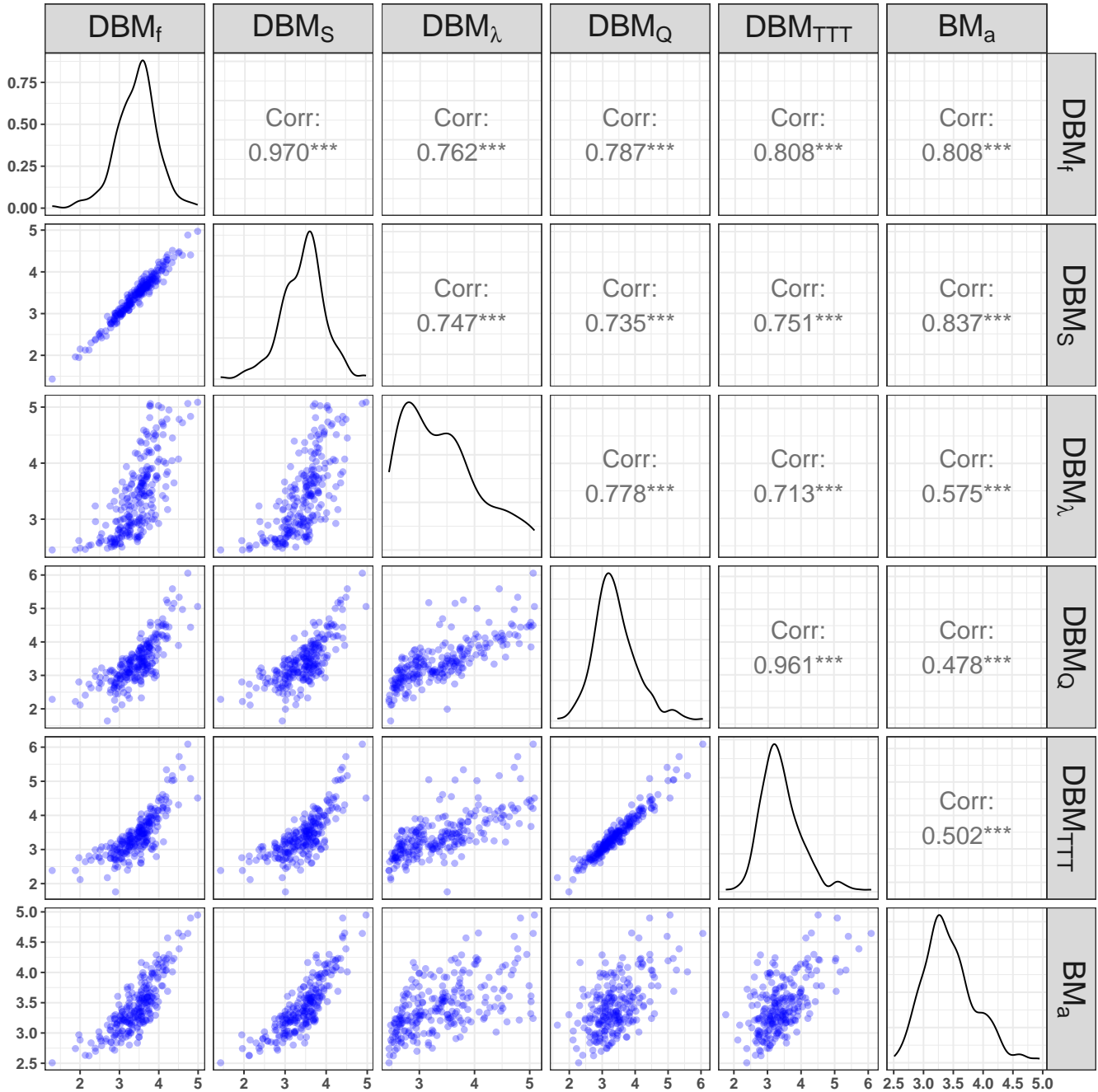


FIGURE 13 Scatter plots of the estimated weighted scores corresponding to the covariates density, survival, hazard, quantile, and TTT functions along with the average physical activity counts to predict EDSS, where the distributional and scalar summaries are obtained based on *log-activity counts*. The upper triangular entries indicate the Spearman's correlation coefficients between the associated row and columns.

TABLE 1 (i) Cross-validated AUCs for binary disability (high vs low EDSS) are shown in columns 2 and 3. (ii) Cross-validated R^2 s for continuous disability (original EDSS scores) are shown in columns 4 and 5. The 95% confidence intervals of are indicated in the parenthesis. All models are described by using the mean function, η_i described in Section 3.

η_i	cross-validated AUC		cross-validated R^2	
	AC in original scale	AC in log scale	AC in original scale	AC in log scale
Scalar summaries as covariates				
$\bar{\beta}_{AC[8am-8pm]} \bar{AC}_{i[8am-8pm]}$	0.70 (0.69, 0.71)	0.65 (0.64, 0.66)	0.13 (0.11, 0.15)	0.10 (0.08, 0.12)
Distribution summaries with domain in quantile levels as covariates				
$\int \bar{\beta}_T(p) \bar{T}_i(p) dp$	0.73 (0.72, 0.75)	0.68 (0.64, 0.71)	0.21 (0.19, 0.23)	0.18 (0.13, 0.22)
$\int \bar{\beta}_Q(p) \bar{Q}_i(p) dp$	0.76 (0.74, 0.77)	0.74 (0.72, 0.76)	0.23 (0.22, 0.25)	0.23 (0.21, 0.26)
Distribution summaries with domain in sample space as covariates				
$\int \bar{\beta}_f(x) \bar{f}_i(x) dx$	0.71 (0.69, 0.73)	0.67 (0.64, 0.69)	0.12 (0.10, 0.15)	0.11 (0.08, 0.14)
$\int \bar{\beta}_S(x) \bar{S}_i(x) dx$	0.72 (0.70, 0.74)	0.69 (0.67, 0.71)	0.12 (0.10, 0.15)	0.12 (0.09, 0.14)
$\int \bar{\beta}_\lambda(x) \bar{\lambda}_i(x) dx$	0.77 (0.76, 0.78)	0.77 (0.76, 0.78)	0.26 (0.23, 0.28)	0.25 (0.24, 0.27)